J Therm Anal Calorim (2012) 109:511–515
DOI 10.1007/s10973-012-2223-8

# The subsolidus area of $CoO–In_2O_3–V_2O_5$ system

**Monika Bosacka**

Bretsznajder Special Chapter


**Abstract** The subsolidus phase relations of the ternary system $CoO–In_2O_3–V_2O_5$ were investigated by differential thermal analysis and X-ray diffraction techniques. It has been shown that the system consists of seven subsidiary systems in which three solid phases coexist in equilibrium. The melting temperatures of these subsystems have also been determined.

**Keywords** Phase equilibria · DTA · $CoO–In_2O_3–V_2O_5$ system · $CoO–In_2O_3$ system

## Introduction

The general aim of the studies is the search for new phases showing properties of cognitive and prospective practical interest. Cobalt metal and its compounds have found a wide range of applications in electrode materials, magnetic materials, chemical catalyst and battery [1–3]. Also indium compounds, in particular indium(III) orthovanadate(V) has been widely used in different branches of industry. $InVO_4$ has been used as an auxiliary material for production of electrodes in cells of different types [4] and as a photocatalyst [5]. Interesting catalytic properties of divalent metal vanadates(V) [6, 7], including cobalt(II) vanadates(V) [1, 3] have been known for many years. It has been established that the catalytic properties of such compounds are related to the presence of isolated $VO_4$ tetrahedrons in them [6, 7]. This finding has prompted us to undertake a comprehensive study of $CoO–In_2O_3–V_2O_5$ system.

Two versions of the $CoO–V_2O_5$ system are known, differing only in the range of stability of the compounds present in the systems and parameters of the eutectic points [8, 9]. As follows from the two diagrams, in the system $CoO–V_2O_5$ there are three cobalt(II) vanadates(V), i.e. $CoV_2O_6$, $Co_2V_2O_7$ and $Co_3V_2O_8$ [8, 9]. Also known is the phase diagram of $In_2O_3–V_2O_5$ system [10] in which in solid state $In_2O_3$ and $V_2O_5$ make only one compound $InVO_4$ [10]. No phase diagram of $CoO–In_2O_3$ and no information on the phases forming in the reaction between the oxides CoO and $In_2O_3$ have been found in the available literature. Only one paper has been come across reporting on formation of a compound in the ternary system $CoO–In_2O_3–V_2O_5$. Previously, the work has studied the reactivity of $Co_2V_2O_7$ towards $InVO_4$ in the solid phase and have proved the formation of a new phase of the formula $Co_2InV_3O_{11}$ [11]. This compound undergoes incongruent melting at 960 °C, and the solid product of melting is $InVO_4$ [11]. The aim of this study was to find out whether in the ternary system $CoO–In_2O_3–V_2O_5$, any other compound, besides $Co_2InV_3O_{11}$, is formed with involvement of all three oxides and to investigate the phase relations in the system studied.

## Experimental

The reagents used in the study came from the following sources

– $V_2O_5$, pure for analysis, made by Riedel-de Haën, Germany

M. Bosacka (✉)
Department of Inorganic and Analytical Chemistry,
West Pomeranian University of Technology,
Al. Piastow 42, Szczecin 71-065, Poland
e-mail: bossm@zut.edu.pl

– $In_2O_3$, pure for analysis, made by Aldrich, Germany
– $CoCO_3$, pure for analysis, Aldrich, Germany

The carefully weighted portions of the reagents were homogenised by milling using agate mortar and heated in the air atmosphere at a few stages until reaching a state of equilibrium. After each stage of heating, the composition of the samples was checked by XRD. The programme of heating (temperatures and duration) was different for individual samples and depended on the composition of initial mixtures.

After the final stage of heating the samples were slowly cooled down to ambient temperature (together with the furnace), and then they were ground and subjected to DTA and XRD measurements. The samples were then heated once again for 24 h at the temperature of the last stage of synthesis and after this time they were rapidly cooled down to room temperature. They were ground once again and studied by DTA and XRD methods. This procedure permitted determination of the types of phases formed in the system studied and the temperature ranges of their co-existence in the solid state [12–14].

DTA measurements were performed on a Metler Toledo $851^e$ apparatus with the samples of 65 mg each placed in quartz crucibles. Measurements were performed in nitrogen atmosphere and at temperatures from the range 500–1,500 °C, at the heating rate of 10°/min.

The phases forming in the samples were identified on the basis of XRD patterns, recorded on a DRON—3 diffractometer, working with $CoK_\alpha$ radiation and Fe filter, and the data from PDF cards [15] and from [11]. Interpretation of XRD patterns was performed with the use of the Program Packing for Powder Diffraction (DHN/PDS).

## Results and discussion

The study began with checking the formation of spinel phases in the $CoO–In_2O_3$ system. For this purpose five mixtures were made of the $CoCO_3/In_2O_3$ molar ratio of 3:1, 2:1, 1:1, 1:2, and 1:3. The samples were heated in the following cycles: at 650 °C(12 h), 750 °C(12 h), 850 °C(12 h), 950 °C(12 h) and additionally at 1,000 °C(3 × 12 h) and 1,100 °C(8 × 7 h). After the last stage of heating the diffractograms of the samples still gave evidence of the presence of $Co_3O_4$ and $In_2O_3$ oxides. $Co_3O_4$ oxide forms as a result of oxidation of cobalt(II) oxide formed on decomposition of $CoCO_3$, [16]. The next set of samples was made of the following $CoCO_3/In_2O_3$ molar ratios: 2:1, 1:1, 1:2 and they were heated in argon atmosphere at 900 °C for 48 h, then cooled down to room temperature under continuous flow of argon. The diffractograms of these samples did not reveal any new diffraction lines besides those characteristic of the oxides CoO, $Co_3O_4$, and $In_2O_3$. The next objective was to establish the phase equilibrium diagram of the subsolidus are of the ternary oxide system $CoO–In_2O_3–V_2O_5$, which was started from investigation of phase relations along the $CoO–InVO_4$ line. Table 1 presents the compositions of initial mixtures, conditions of their heating and XRD results obtained for the samples after the last stage of heating.

XRD analysis of the samples obtained from the initial mixtures containing 90.00, 80.00, 70.00 and 66.67% mol CoO has shown the presence of three phases $In_2O_3$, $Co_3V_2O_8$ and $Co_3O_4$. The presence of $Co_3O_4$ follows from the fact that cobalt(II) oxide does not exist below 900 °C because it is oxidised [17]. In the sample corresponding to the initial $CoO/InVO_4$ molar ratio of 3:2 two phases $In_2O_3$ and $Co_3V_2O_8$ were identified. The other samples formed from the initial mixtures containing 55.00, 50.00, 40.00,

**Table 1** The composition, the heating conditions, and the kind of phases detected after the last heating stage in the samples from the system $CoO–InVO_4$

| No | Contents/mol%/ | | The heating temperature and time | The composition of the sample in an equilibrium state |
|---|---|---|---|---|
| | CoO | $InVO_4$ | | |
| 1 | 10.00 | 90.00 | 450–550 °C/24 h + 650 °C/24 h + 750 °C/24 h | $InVO_4$, $In_2O_3$, $Co_3V_2O_8$ |
| 2 | 20.00 | 80.00 | 800 °C/24 h + 850 °C/2 × 24 h + 900 °C/2 × 24 h | |
| 3 | 30.00 | 70.00 | | |
| 4 | 40.00 | 60.00 | | |
| 5 | 50.00 | 50.00 | | |
| 6 | 55.00 | 45.00 | | |
| 7 | 60.00 | 40.00 | | $In_2O_3$, $Co_3V_2O_8$ |
| 8 | 66.67 | 33.33 | | $In_2O_3$, $Co_3V_2O_8$, $Co_3O_4$ |
| 9 | 70.00 | 30.00 | | |
| 10 | 80.00 | 20.00 | | |
| 11 | 90.00 | 10.00 | | |

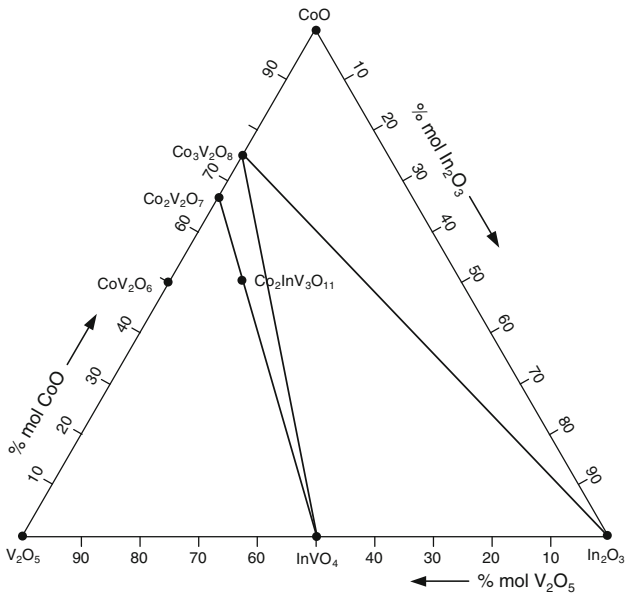


**Fig. 1** Preliminary division of the investigated ternary CoO–$In_2O_3$–$V_2O_5$ systems into subsidiary subsystem

30.00, 20.00, and 10.00% mol CoO, were composed of $InVO_4$, $In_2O_3$ and $Co_3V_2O_8$.

As follows from the results obtained, the system CoO–$InVO_4$ is not a real binary system but it is an intersection of the ternary oxide system CoO–$V_2O_5$–$In_2O_3$. It has been earlier established that the intersection $Co_2V_2O_7$–$InVO_4$ of the ternary system in the subsolidus area is a real binary system in the whole concentration range of components in which $Co_2InV_3O_{11}$ undergoes crystallisation [11]. On the basis of the data from Table 1, from the phase equilibrium diagram in the intersection $Co_2V_2O_7$–$InVO_4$ [11] and from the phase diagrams of CoO–$V_2O_5$ [9] and $In_2O_3$–$V_2O_5$ [10] it was possible to propose a preliminary division of the subsolidus area of CoO–$In_2O_3$–$V_2O_5$ into the regions corresponding to subsidiary subsystems (Fig. 1). Regarding the fact that diffractograms of the samples were taken at room temperature and taking into account that thermal decomposition of $Co_3O_4$ takes place at about 900 °C [17] it was concluded that the phase diagram represented the region corresponding to the compounds: CoO–$In_2O_3$–$Co_3V_2O_8$.

The division proposed did not include the polygon whose apices corresponded to the compounds $V_2O_5$, $CoV_2O_6$, $Co_2V_2O_7$, $Co_2InV_3O_{11}$ and $InVO_4$. In order to establish the phase relations in this polygon and to verify the predicted partial systems in the other area of the system CoO–$In_2O_3$–$V_2O_5$. The mixtures of $CoCO_3$, $V_2O_5$ and $In_2O_3$ were prepared of the compositions chosen to represent the ranges hitherto not studied and some hypothetical partial systems comprised in the oxide systems studied. The compositions of initial mixtures from which the second series samples were obtained, the stages of heating and phases detected in the equilibrium state are given in Table 2.

In order to find out the melting points of the binary and ternary systems forming in the ternary oxide system CoO–$In_2O_3$–$V_2O_5$, all samples were subjected to DTA analysis. Figure 2 presents selected DTA curves recorded for the

**Table 2** The composition, the heating stages, and the kind of phases identified after the final heating stage of selected samples lying within the binary or ternary subsystems

| No | Contents/mol%/ | | | The heating temperature and time | The phase composition of the sample in an equilibrium state |
|---|---|---|---|---|---|
| | CoO | $In_2O_3$ | $V_2O_5$ | | |
| 1 | 20.00 | 15.00 | 65.00 | 500 °C/12 h + 550 °C/12 h + 590 °C/2 × 12 h + 600 °C/2 × 12 h + 610 °C/12 h | $InVO_4$, N-$CoV_2O_6$, $V_2O_5$ |
| 2 | 37.00 | 13.00 | 50.00 | | |
| 3 | 25.00 | 25.00 | 50.00 | 500 °C/12 h + 550 °C/12 h + 600 °C/12 h + 700 °C/2 × 12 h | $InVO_4$, N-$CoV_2O_6$ |
| 4 | 40.00 | 15.00 | 45.00 | | N-$CoV_2O_6$, $InVO_4$, $Co_2InV_3O_{11}$ |
| 5 | 30.00 | 25.00 | 45.00 | | |
| 6 | 50.00 | 5.00 | 45.00 | | N-$CoV_2O_6$, $Co_2InV_3O_{11}$ |
| 7 | 35.00 | 15.00 | 50.00 | | |
| 8 | 55.00 | 5.00 | 40.00 | | N-$CoV_2O_6$, $Co_2V_2O_7$, $Co_2InV_3O_{11}$ |
| 9 | 61.00 | 2.00 | 37.00 | | |
| 10 | 61.00 | 5.00 | 34.00 | 500 °C/12 h + 550 °C/12 h + 600 °C/12 h + 700 °C/2 × 12 h + 750 °C/2 × 12 h | $Co_3V_2O_8$, $Co_2InV_3O_{11}$, $Co_2V_2O_7$ |
| 11 | 65.00 | 3.00 | 32.00 | | |
| 12 | 65.00 | 5.00 | 30.00 | 500 °C/12 h + 550 °C/12 h + 650 °C/12 h + 750 °C/2 × 12 h + 850 °C/12 h + 900 °C/2 × 12 h | $Co_2InV_3O_{11}$, $Co_3V_2O_8$ |
| 13 | 50.00 | 15.00 | 35.00 | | $Co_2InV_3O_{11}$, $InVO_4$, $Co_3V_2O_8$ |
| 14 | 60.00 | 10.00 | 30.00 | | $Co_3V_2O_8$, $InVO_4$ |
| 15 | 65.00 | 10.00 | 25.00 | | $Co_3V_2O_8$, $InVO_4$, $In_2O_3$ |
| 16 | 30.00 | 45.00 | 25.00 | | |

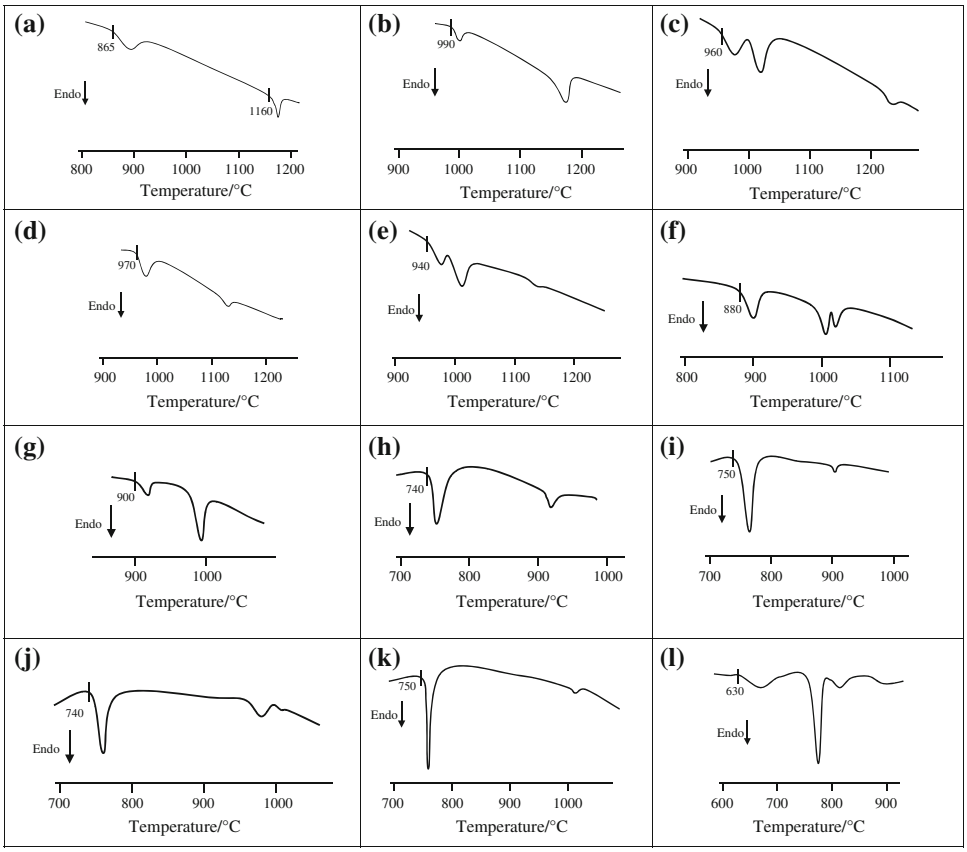


**Fig. 2** DTA curves of selected samples at representing equilibrium: **a** subsidiary system $CoO–Co_3V_2O_8–In_2O_3$, **b** binary system $Co_3V_2O_8–In_2O_3$, **c** subsidiary system $Co_3V_2O_8–In_2O_3–InVO_4$, **d** binary system $Co_3V_2O_8–InVO_4$, **e** subsidiary system $Co_3V_2O_8–Co_2InV_3O_{11}–InVO_4$, **f** subsidiary system $Co_3V_2O_8–Co_2V_2O_7–Co_2InV_3O_{11}$, **g** binary system $Co_3V_2O_8–Co_2InV_3O_{11}$, **h** subsidiary system $Co_2V_2O_7–Co_2InV_3O_{11}–CoV_2O_6$, **i** binary system $CoV_2O_6–Co_2InV_3O_{11}$, **j** subsidiary system $CoV_2O_6–Co_2InV_3O_{11}–InVO_4$, **k** binary system $CoV_2O_6–InVO_4$ and **l** subsidiary system $CoV_2O_6–V_2O_5–InVO_4$

samples representing partial binary and ternary systems of the main system studied. The melting points of the mixtures of phases were determined as the temperatures of the beginning of the first endothermic effects not corresponding to polymorphous transformations, detected on DTA curves. Figure 2a presents the DTA curve of the sample from $CoO–In_2O_3–Co_3V_2O_8$ system. The first endothermic effect was recorded at 865 °C and interpreted as corresponding to decomposition of $Co_3O_4$ to CoO [17]. The second endothermic effect on this DTA curve beginning at 1160 °C, probably corresponds to the melting point of the ternary mixture.

On the basis of the results obtained and literature data [9–11], the phase diagram of the subsolidus area of the ternary oxide system $CoO–In_2O_3–V_2O_5$ was proposed, Fig. 3. The same figure also shows the melting points of the mixtures of phases at equilibrium and representing the partial systems and the intersections standing for the conjugation lines, i.e., the real binary intersections.

According to the phase diagram presented in Fig. 3, seven partial systems can be distinguished in the $CoO–In_2O_3–V_2O_5$ system, and in each of them three solid phases coexist. The partial systems were identified as follows.

I $CoO–In_2O_3–Co_3V_2O_8$
II $Co_3V_2O_8–In_2O_3–InVO_4$

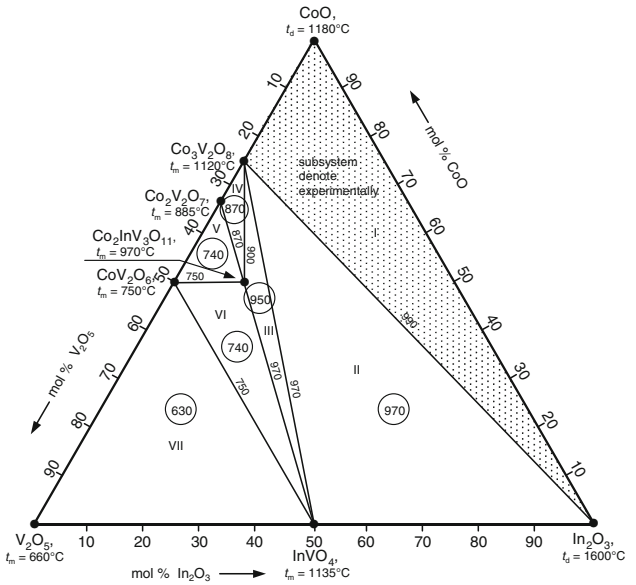


**Fig. 3** A division of the component concentration triangle of the system $CoO–In_2O_3–V_2O_5$ into partial subsystems and the melting temperatures of the subsidiary systems and binary systems

III $Co_3V_2O_8–InVO_4–Co_2InV_3O_{11}$
IV $Co_3V_2O_8–Co_2V_2O_7–Co_2InV_3O_{11}$
V $Co_2V_2O_7–Co_2InV_3O_{11}–CoV_2O_6$

VI $CoV_2O_6$–$Co_2InV_3O_{11}$–$InVO_4$
VII $CoV_2O_6$–$InVO_4$–$V_2O_5$

## Conclusions

As a result of a solid state reaction in the binary system CoO–$In_2O_3$ no phases are formed. In the ternary system CoO–$In_2O_3$–$V_2O_5$ only one compound of the formula $Co_2InV_3O_{11}$ is formed with the involvement of all three oxides. On the basis of the measurements performed the phase equilibrium diagram has been proposed for the ternary system CoO–$In_2O_3$–$V_2O_5$ in the subsolidus area. It has been found that seven partial systems can be distinguished in the main system studied.



## References

1. Cowin PI, Lan R, Petit ChTG, Zhang L, Tao S. Conductivity and stability of cobalt pyrovanadate. J Alloys Compd. 2011;50: 4117–21.
2. Wilczkowska E, Krawczyk K, Petryk J, Sobczak JW, Kaszkur Z. Direct nitrous oxide decomposition with a cobalt oxide catalyst. Appl Catal A. 2010;389:165–72.
3. El-Shobaky GA, El-Mohsen A, Turky M. Catalytic decomposition of $H_2O_2$ on $Co_3O_4$ doped with MgO and $V_2O_5$. Colloids Surf A. 2000;170:161–72.
4. Xiao G, Wang X, Li D, Fu X. $InVO_4$-sensitized $TiO_2$ photocatalysis for efficient air purification with visible light. J Photochem Photobiol A Chem. 2008;193:213–21.
5. Enache CS, Lioyd D, Damen MR, Schoonman J, van de Krol R. Photo-electrochemical properties of thin-film $InVO_4$ photoanodes: the role of deep donor state. J Phys Chem C. 2009;113: 19351–60.
6. Charr MA, Patel D, King MC, Kung HH. Selective oxidative dehydrogenation of butane over V–Mg–O catalysts. J Catal. 1987;105: 483–98.
7. Pless JD, Bardin BB, Kim H-S, Ko D, Smith MT, Hammond RR, Stair PC, Poeppelmeier KR. Catalytic oxidative dehydrogenation of propane over Mg–V/Mo oxides. J Catal. 2004;223:419–31.
8. Brisi C. The systems nickel oxide—vanadic anhydride and cobaltous oxide—vanadic anhydride. Ann Chim (Roma). 1957;47: 806–16.
9. Fotiev AA, Slobodin BV, Khodos Ya M. Vanadaty: sostav, sintez, strukturam svoistva. Izd Nauka Moskwa. 1988.
10. Touboul M, Melighit K. Synthesis by "chimie douce" and characterization of indium vanadates. Eur J Solid State Inorg Chem. 1994;31:151–61.
11. Bosacka M. The synthesis and selected properties of $Co_2InV_3O_{11}$. J Therm Anal Cal. 2007;88:43–6.
12. Blonska-Tabero A. Subsolidus area of the system CdO–$V_2O_5$–$Fe_2O_3$. Cent Eur J Chem. 2009;7(2):252–8.
13. Filipek E, Piz M. The reactivity of $SbVO_5$ with T-$Nb_2O_5$ in solid state in air. J Therm Anal Cal. 2010;101:447–53.
14. Tabero P. Formation and properties of new $Al_8V_{10}W_{16}O_{85}$ and $Fe_{8-x}Al_xV_{10}W_{16}O_{85}$ phases with the M-$Nb_2O_5$ structure. J Therm Anal Cal. 2010;101:561–6.
15. Powder Difraktion File, International Center for Diffraction Data, Swarthmore (USA), File Nos.: 06-0416, 09-0387, 09-402, 09-418, 11-0692, 33-0628, 37-0352, 38-0090, 38-0252.
16. Blonska-Tabero A. Phase relations in the CoO–$V_2O_5$–$Fe_2O_3$ system in subsolidus area. J Therm Anal Cal. 2007;88:201–5.
17. Shaheen WM, Selim MM. Thermal characterization and catalytic properties of the ZnO–$Co_3O_4$/$Al_2O_3$ system. Int J Inorg Mater. 2001;3:417–25.